



ELSEVIER

Available online at www.sciencedirect.com

SCIENCE @ DIRECT®

Nuclear Instruments and Methods in Physics Research B 205 (2003) 700–704

NIM B
Beam Interactions
with Materials & Atomswww.elsevier.com/locate/nimb

Projectile neutralization in large-angle back-scattering of slow F^{q+} , Ne^{q+} and Ar^{q+} incident on $RbI(100)$

F.W. Meyer ^{*}, H.F. Krause, C.R. Vane*Physics Division, Oak Ridge National Laboratory, Oak Ridge, TN 37831-6372, USA*

Abstract

The scattering of multi-charged ions (MCI) from the [1 0 0] surface of a RbI single crystal has been studied using a 120° back-scattering technique in the keV energy regime. Scattered charge-state distributions were measured as a function of the polar incidence angle and the target azimuthal orientation. Preliminary results indicate that “quasi-binary” collisions associated with scattering from a Rb or I site can be clearly distinguished for each scattered final charge state. The charge-state distribution and the relative Rb/I binary collision yields for scattered ions are found to depend on both the beam incidence angle and the target azimuthal orientation. The preliminary RbI(1 0 0) results are discussed in the context of earlier experimental and theoretical studies of MCI scattering on a Au(1 1 0) surface.

© 2002 Elsevier Science B.V. All rights reserved.

PACS: 79.20.Rf; 79.20.Ap; 34.50.Dy; 61.18.Bn

Keywords: Ion-surface scattering; Highly charged projectile neutralization; RbI; Multi-charged ions

1. Introduction

The large-angle back-scattering technique has seen increased use in studies of multi-charged ions (MCI) neutralization during interactions with solid surfaces [1–7]. In contrast to grazing incidence studies where a large number of lattice sites are involved [8], large-angle back-scattering measurements allow the resolution of interactions occurring with just one or two atoms located on the target surface. Furthermore, the use of MCI projectiles has been shown to significantly enhance the surface sensitivity of the back-scattering technique [3].

Simultaneous energy and charge-state analysis of the back-scattered projectiles have provided insights into energy loss mechanisms accompanying projectile neutralization leading to particular final charge states [1,2]. More recently, the large-angle back-scattering technique has provided information on site-specific MCI neutralization at a Au(1 1 0) surface. In the latter work, a strong target azimuth dependence was observed in the scattered projectile charge state distributions. Extensive trajectory simulations performed in conjunction with the measurements were able to reproduce the observed variations with target azimuth, and provided a framework for demonstrating differences in MCI neutralization at the different possible scattering sites on the corrugated Au(1 1 0) metal surface [3,7].

^{*} Corresponding author. Fax.: +1-865-574-1118.

E-mail address: meyerfw@ornl.gov (F.W. Meyer).

We have recently extended such studies to insulator targets by measuring projectile back-scattering from RbI(100). Goals of this work are to identify and understand differences in final charge-state distributions and neutralization mechanisms that occur on ordered insulator and metal surfaces. RbI(100) was chosen in the hope of obtaining site-resolved projectile neutralization information at Rb and I lattice sites. Due to their significant mass difference, large-angle back-scattering from the two lattice sites should lead to sufficiently different elastic binary collision energy losses to be resolvable by our time-of-flight (TOF) energy analysis technique.

2. Experiment

The measurements were performed at the ORNL Multi-charged Ion Research Facility using an ultra high vacuum (10^{-10} mbar) apparatus previously described [2]. A chopped primary ion beam (Ar^{q+} , Ne^{q+} , or F^{q+}) is decelerated from $(10 \times q)$ keV to final energies in the range 2–10 keV before impinging on the crystal surface. The crystal is attached to a goniometer that has two rotational degrees of freedom. A TOF analyzer, located 120° from the incident beam direction, measures pulsed ions scattered from the crystal surface. The TOF analyzer, which has a floatable drift tube, allows simultaneous measurement of energy distributions and charge fractions for the scattered ions [2]. The RbI(100) surface was prepared by cycles of sputter cleaning under grazing incidence conditions using 2 keV Ar^+ ions and successive annealing at about 450°C . To prevent macroscopic charging, the RbI target was maintained at a temperature of 250°C during the measurements.

The energy-loss technique enables identification of different collision sequences occurring at the surface. When a projectile of energy E_0 (mass = m_p) elastically scatters from a target atom at rest (mass = m_t), the projectile recoil energy E_r depends on the scattering angle θ as

$$E_r = E_0 \left\{ \left[\mu \cos \theta + (1 - \mu^2 \sin^2 \theta)^{1/2} \right] / (1 + \mu) \right\}^2, \quad (1)$$

where $\mu = m_p/m_t < 1$. A 120° scattering event (“hard” collision), which is associated with a small impact parameter collision (e.g. $\rho_b \sim 0.004$ nm), results in a substantial energy loss. When the surface has two constituents of significantly different mass (e.g. Rb and I), hard collisions at the two sites give rise to different recoil energies that can be resolved experimentally in our TOF apparatus (site specificity for each final charge state). In contrast, for a subsequent small-angle scattering event (i.e. “soft” collision, $\rho \gg \rho_b$), very little energy is lost in a collision with either Rb or I. Therefore, a “quasi-binary” double scattering event (“hard–soft” collision sequence) can have an energy loss close to that of a single “hard” collision. Interesting possibilities arise when an ionic crystal such as RbI is examined with this technique.

RbI has a diatomic cubic structure (rock salt) of alternating atoms ABAB on each side of the unit cell (e.g. a $\langle 100 \rangle$ direction, 0.366 nm atomic spacing). In a $\langle 110 \rangle$ direction, there are alternating parallel rows AAAA and BBBB (0.517 nm atomic spacing). Thus, azimuthal rotation of the crystal (e.g. alignment of a $\langle 100 \rangle$ or a $\langle 110 \rangle$ direction to the scattering plane) changes the adjacent atomic species and their atomic spacing. Moreover, interaction with widely spaced A_B_A_B atomic strings (0.818 nm spacing) can be measured when a $\langle 210 \rangle$ direction is selected. In the experiment, the relative intensities for binary scattering associated with Rb and I sites provide a “signature” for identifying and probing neutralization pathways in these different orientation-dependent “quasi-binary” collision sequences.

3. Results

Collisions of F^{q+} ($q = 1, 2, 6$ and 7), Ne^{q+} ($q = 8$ and 9) and Ar^{q+} ($q = 9, 11$) incident on a RbI(100) surface were studied in the 2–10 keV energy regime. Scattered projectile charge-state distributions were determined as a function of incident polar angle, θ and azimuthal orientation angle, Φ . Raw TOF spectra in Fig. 1 illustrate the polar incidence angle dependence for the F^0 and F^+ yields, when 4.2 keV F^+ ions (simplest possibility) are

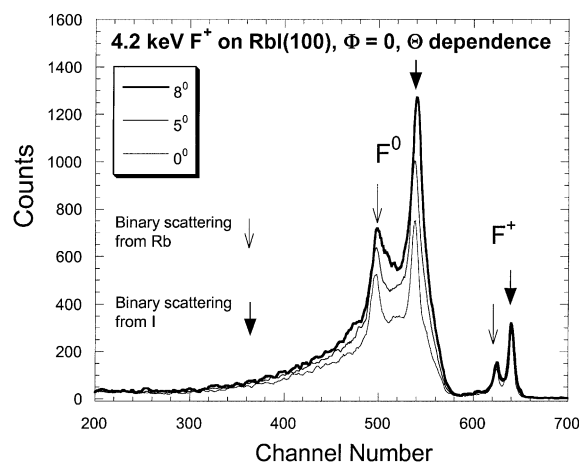


Fig. 1. Raw TOF spectra showing polar incidence angle dependence of the flux of F^0 and F^+ ions for 4.2 keV F^+ ions 120° back-scattered from RbI(100) along the $\langle 100 \rangle$ direction; 0° corresponds to normal incidence. Time increases from right to left; $10\text{ ns} = 657$ channels.

scattered along a $\langle 100 \rangle$ direction of RbI (different adjacent atomic sites). Binary peaks associated with Rb and I sites are clearly resolved for both the neutral and 1+ final charge states (left and right doublets, respectively). The TOF separation for each binary peak agrees with calculated times using the known TOF geometry, applied bias voltages, and the recoil energies from Rb and I predicted by Eq. (1). We see that the F^0 yield increases strongly as θ increases from normal incidence in a direction toward more grazing exit angles, while the F^+ yields are essentially independent of θ . This observation suggests that the increased back-scattering flux resulting from participation of layers below the surface when they become “unblocked” (i.e. not hidden below the top layer) away from normal incidence is comprised almost entirely of F^0 , while the surviving F^+ charge fraction is entirely due to interaction with the surface layer. As is evident from the figure, the increased F^0 flux away from normal incidence is comprised both of an increasing broad background due to multiple collisions and an increasing area of the narrower binary collision peaks. Interestingly, the Rb/I binary peak ratio for the 1+ charge state in Fig. 1 (F^+ incident ions) agrees approximately with that measured for incident F^{7+}

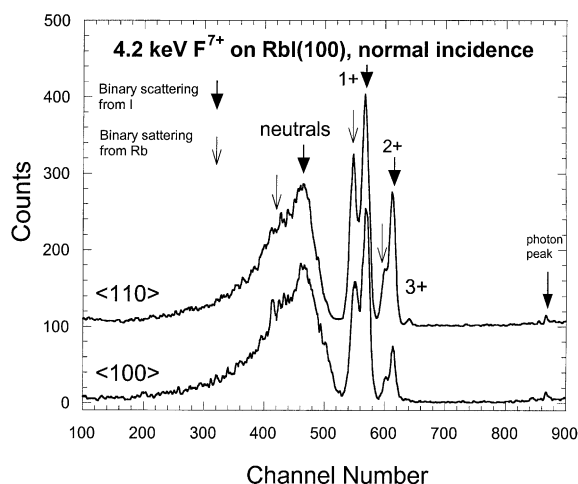


Fig. 2. Raw TOF spectra for normal incidence 4.2 keV F^{7+} ions scattered along $\langle 100 \rangle$ and $\langle 110 \rangle$ directions of RbI(100); $t = 0$ is determined from photon peak at channel 870.

ions in the same $\langle 100 \rangle$ crystal orientation (see Fig. 2). Tilt spectra for other MCI species exhibit similar characteristics, except that the doublet binary peaks for incident Ar^{11+} ions were not cleanly resolved, as will be discussed in greater detail below.

Our data indicate that the measured charge-state distributions and the Rb/I binary peak intensity ratio for each charge state depend on the azimuthal orientation of the crystal, even for projectile impact normal to the surface. Fig. 2 shows the large variation in the scattered charge fractions when 4.2 keV F^{7+} ions are normally incident, (i.e. in the “blocking” direction, $\theta = 0$) as the crystal azimuth is rotated. Comparing Fig. 2 spectra recorded when the scattering plane is aligned to either the $\langle 110 \rangle$ or the $\langle 100 \rangle$ direction, we see that the $\langle 110 \rangle$ orientation (upper trace) yields a higher average final charge state. The binary fractions associated with Rb or I scattering also vary for each charge state and orientation. In fact, the measured Rb/I binary ratio for F^+ (~ 0.7) agrees with the ratio of screened Coulomb classical differential binary scattering cross sections [9], but only in the $\langle 110 \rangle$ orientation. Perhaps F^+ formation along $\langle 110 \rangle$ is dominated by single binary scattering because adjacent atoms are farther apart in this orientation. Quasi-binary double collisions [3] might be expected to cause the binary ratio to

deviate from the calculated value of 0.7. For the other crystal orientation and other charge states, “quasi-binary” collisions of the Rb–Rb or I–I type along $\langle 110 \rangle$ and Rb–I or I–Rb sequences along the $\langle 100 \rangle$ direction may account for the different measured binary ratios (i.e. scrambled binary ratios, including the Rb/I < 0.7 ratio shown in Fig. 1 for the scattered $1+$ charge state). Azimuthal variations caused by “quasi-binary” double collisions on Au(110) were clearly identified in our previous studies [3,7].

Another feature of the raw spectra shown in Fig. 2 is the strongly reduced binary collision neutral peaks in comparison with the F^+ incident ion spectra of Fig. 1 which features prominent binary collision neutral components. This is a shared feature of all the spectra measured for MCI incident on RbI(100), as well as of our earlier measurements on CsI(100) [6]. This feature is in strong contrast to our measurements on Au(110), where binary collision neutrals were the dominant scattered charge state for all incident charge states investigated [3,7].

Absence of a significant binary collision neutral peak is more obvious in Fig. 3 which shows raw back-scattering spectra for 4.8 Ne $^{8+}$ normally incident on RbI(100) for two different target azimuths. The photon peaks around channel 670 used for the $t = 0$ calibration are more prominent in these spectra as well. Again, as in the case of the F^{7+} spectra shown in Fig. 2, there are significant azimuth variations in the intensities of the scattered charge states, which extend to $3+$ for Ne $^{8+}$ ions, and in the Rb/I collision peak ratios. More quantitative conclusions and results will be derived from the measured spectra after they have been corrected for collection and detection efficiencies of the different charge states using procedures outlined in [2].

Fig. 4 shows raw back-scattering spectra for 7 keV Ar $^{11+}$ projectiles incident on RbI(100) normally and at 30° from normal. Spectra obtained for TOF drift tube voltages of -2 and 0 kV illustrate the effect of charge state dispersion when the drift tube is at high voltage. With the drift tube grounded, all scattered charge states collapse into a single peak (\sim channel 440 in the figure). In contrast to the spectra shown in the previous fig-

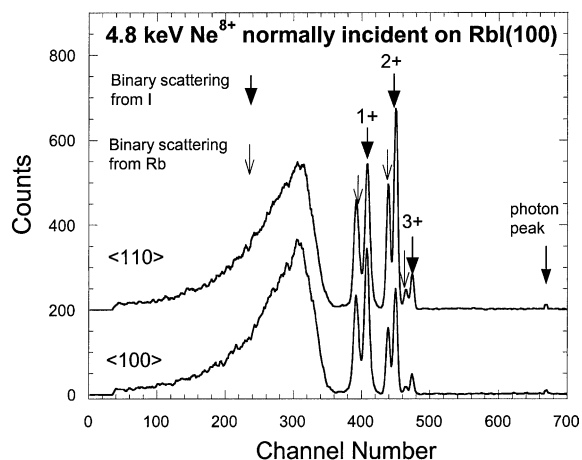


Fig. 3. Raw TOF spectra for normal incidence 4.8 keV Ne $^{8+}$ ions scattered along $\langle 100 \rangle$ and $\langle 110 \rangle$ directions of RbI(100).

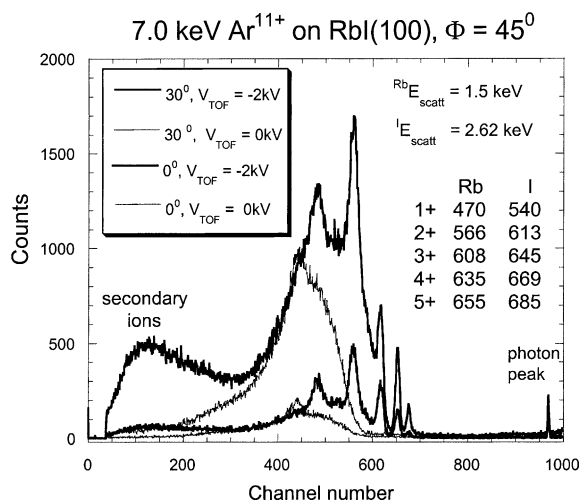


Fig. 4. Raw spectra for 7 keV Ar $^{11+}$ ions incident on RbI(100) for two different incidence angles along the $\langle 110 \rangle$ direction. $V = 0$ kV and $V = -2$ kV drift tube conditions are shown for both cases. The inset tabulates the calculated channel numbers for the different scattered charge states originating from hard collisions with Rb and I sites.

ures, there is no clean separation of binary scattering from Rb and I. As the inset in the figure shows, the channel separation of the binary collision peaks originating from Rb and I sites are comparable to the peak separation of the different scattered charge states. Thus, making unique

identification of the observed peaks in the absence of more detailed analysis is difficult for this case. This smearing effect is due to the relatively lower back-scattered projectile energies (due to the larger projectile/target mass ratio (see Eq. (1)) in relation to the applied drift tube voltage.

4. Summary

Our preliminary results for projectile back-scattering from RbI(100) indicate that, with exception of the 1+ incident charge state shown in Fig. 1, the majority of back-scattered projectiles are charged. This finding contrasts with our Au(110) results showing most of the yield is in the neutral channel. One possible reason for the decreased neutralization observed for this target is that the collision time may be significantly shorter than the lattice-site reneutralization time (“hole hopping” time [11]). In addition, significant target azimuth dependences are seen both for the Rb/I binary collision peak ratios and the scattered charge state distributions arising from a given lattice site. In analogy with the Au(110) studies, most RbI azimuthal effects probably arise from “hard–soft” quasi-binary double collision sequences. To disentangle the various possible quasi-binary collision combinations leading to the observed azimuth variations of the binary collision energy-loss peaks, detailed MARLOWE trajectory simulations [10] are planned using the same for-

malism and approach developed previously for the analysis of our Au(110) results.

Acknowledgements

This research was sponsored in part by the Office of Fusion Energy Sciences and by the Office of Basic Energy Sciences of the US Department of Energy under contract no. DE-AC05-00OR22725 with UT-Battelle, LLC.

References

- [1] W. Huang, H. Lebius, R. Schuch, M. Grether, N. Stolterfoht, *Phys. Rev. A* 58 (1998) 2962.
- [2] V.A. Morozov, F.W. Meyer, *Rev. Sci. Instr.* 70 (1999) 4515.
- [3] V.A. Morozov, F.W. Meyer, *Phys. Rev. Lett.* 86 (2001) 736.
- [4] V.A. Morozov, F.W. Meyer, *Phys. Scr. T* 92 (2001) 31.
- [5] F.W. Meyer, V.A. Morozov, R.C. Vane, S. Datz, *Phys. Scr. T* 92 (2001) 182.
- [6] F.W. Meyer, V.A. Morozov, J. Mrogenda, C.R. Vane, S. Datz, *Nucl. Instr. and Meth. B* 193 (2002) 508.
- [7] F.W. Meyer, V.A. Morozov, *Nucl. Instr. and Meth. B* 193 (2002) 530.
- [8] F.W. Meyer, Q. Yan, P. Zeijlmans van Emmichoven, I.G. Hughes, G. Spierings, *Nucl. Instr. and Meth. B* 125 (1997) 138.
- [9] M.T. Robinson, *Tables of Classical Scattering Integrals*, ORNL-4556, 1970.
- [10] M.T. Robinson, *Radiat. Eff. Def. Solid* 130 (1994) 3.
- [11] L. Wirtz, C. Lemell, C.O. Reinhold, L. Hägg, J. Burgórfer, *Nucl. Instr. and Meth. B* 182 (2001) 36.